Journal of Analytical Chromatography and Spectroscopy (2018)

ORIGINAL RESEARCH ARTICLE

Comparison of Wet Deposition and Plasma Deposition of Aluminosilane Coatings

Shunxing Qi,Haiyan Li,Yu Chen

College of Chemistry and Chemical Engineering, Hohhot University of Technology, Inner Mongolia,
China

ABSTRACT

Silane coatings are suitable for various applications of metal surfaces, such as forming a corrosion protection layer or as a primer for subsequent coating. In this work, bis-1,2- (triethoxy) ethane (BTSE) was used as a precursor on a 99.99% aluminum substrate for deposition of the coating, with three diff erent techniques: dipping (water-based solution), Vacuum plasma and atmospheric plasma. (IRRAS), X-ray photoelectron spectroscopy (XPS) and fi eld emission gun scanning electron microscopy (FE-SEM) were used to characterize the structure, composition and surface morphology of silane coating. The purpose of this study is to compare the surface and body properties of membranes prepared by three different methods to obtain information on how BTSE molecules are modified by deposition techniques. The results show that in addition to the more traditional wet dip coating, the film can also be vacuum and atmospheric plasma deposition. The vacuum plasma deposition layer can be considered as an organic and inorganic mixture, which can be obtained by dipping as well as the silane layer. However, atmospheric plasma treatment leads to the formation of more inorganic fi lms containing Si-O. Photon spectroscopy and infrared spectroscopy showed the presence of Si-O-Si bonds, while IRRAS measurements showed Si-O-Si, Si-O-C, Si-O and Si-CH3 absorption bands.

KEYWORDS: plasma deposition, silane, BTSE, X-ray photoelectron spectroscopy, IRRAS

1. Introduction

In various applications, the metal surface covers the organic film to improve its overall performance, especially its corrosion performance. A variety of silanes have been studied by dip coating for aluminum and alloy steels [1,2]. Silane provides a strong substrate adhesion, in the aluminum alloy to show outstanding corrosion protection performance. In some cases the equivalent of hexavalent chromium containing conversion pretreatment [3]. It has been found that non-functional silanes such as di-1, 2- (triethoxy) ethane (BTSE) are more effective than organic functional silanes such as γ-aminopropyltriethoxysilane (γ-APS) [4] and Γ-glycidoxypropyltrimethoxysilane (γ-GPS) [5] showed better corrosion protection performance. Silane film deposition coating process can be dry or wet, depending on the method of use [6-8]. Up to now, most of these silane films have been deposited from the solution by dip coating or sticky rolls, which requires the addition of water to the silane molecules to hydrolyze the methoxy or ethoxy groups and form functional methyl groups,

(1)Wherein X represents an organic functional group such as chlorine, amine, epoxy or mercapto. An important aspect of the surface of the metal-containing silane is the nature of the matrix and the pretreatment. The formation of hydroxyl groups on the metal surface requires an alkaline pretreatment, along with the silanol components, which are essential for the formation of the covalent Si-O-metal bond at the metal / film interface [9,10]. In addition, the heat treatment of the silane film improves the protective properties [10] by enhancing the crosslinking (condensation of the silanol component).

(2)This cross-linking film will then be used as a physical barrier between the metal matrix and the aggressive environment by reducing the number of possible permeation paths. Therefore, the protective properties of the film and the corrosion resistance of the substrate are improved.

In order to improve the BTSE coating preservative additives are contained in the silane matrix, both for the barrier and for the corrosion inhibition enhancement [11-15]. A recent study by Phanasgaonkar and Raja [16] and Montemor et al. [17] demonstrated that the addition of silica nanoparticles to the silane film will increase the corrosion resistance of the coating. The nanoparticles enhance the formation of crack-free membranes while improving mechanical durability and corrosion resistance [18]. They also appear to have clogging effects [19-21] because they can fill defects and voids

in the silane film. This results in a significant decrease in porosity and conductivity, which also improves the protective properties. The wet deposition of silanes is being studied extensively, but the technology exhibits some drawbacks. First, wet deposition is a multistage treatment that requires a special substrate to be pre-treated in the deposition film to enhance the adhesion of the metal film and a post-treatment by heat curing to improve the protective properties. In addition, the wet treatment involves the use of the solution (if not based on water containing organic solvents, i.e., n-hexane, acetone and ethanol) and the manufacture of waste streams. In addition to the long time (about two days) required to hydrolyze the coating solution [22], it is also possible that some water or solvent remains in the silane film after curing, which reduces corrosion resistance.

The plasma technology is an effective and good substitute for wet settling, which allows the plasma cleaning step to be carried out before the polymer is deposited on the same reaction. The plasma is used to chemically decompose the precursor silane vapor and serve as a source of active species involved in membrane growth. The plasma polymerization process is usually carried out at low pressure, and the main drawback of this process in industrial applications is the high cost of the vacuum system and the limitations of the vacuum-enclosed reaction, which makes the sample more difficult to prepare continuously. In order to develop alternative techniques to overcome these shortcomings, the researchers paid a considerable effort. Atmospheric plasma is one of the most promising ways to settle polymer films in a more flexible, reliable, low-cost, continuous manner [23].

Plasma deposition of some silane films has been studied [8]. Most of these studies describe the properties of the structure and the properties of the deposited polymer films [24-28] and are accompanied by the mechanism of the plasma polymerization mechanism of organosilicon compounds [29,30]. These films act as corrosion protection coatings because they are usually branched, highly crosslinked, insoluble, pinhole-free, and highly adherent to most substrates [31, 32]. The silane layer acts as an interface modifier to improve adhesion and corrosion resistance.

Recent studies have been performed on 99.99% aluminum silane (BTSE) membrane surfaces and chemically described to obtain different deposition methods: dip coating (water based), vacuum and atmospheric plasmas. The plasma polymerization of BTSE has never been reported in previous studies and there are no available reports on the comparison of different deposition methods. It is observed that the initial results of the same coating and how the different properties depend on the technology used.

2. Experiment

The coatings were deposited on high purity aluminum sheets (aluminum 99.99%), alkaline pretreated substrates, and the surface was activated by immersing them in NaOH solution (25 g / l at 343 K) for 6 seconds and then rinsed with water , With pressurized air drying.

Pioneer Study (Bis-1,2- (triethoxy) ethane) BTSE: Dilute with 10% water-based solution and concentrate 98% pure solution with plasma deposition. Both solutions are supplied by the German company. The molecular structure of BTSE (CH2) 2Si2 (OC2H5) 6 is shown in Figure 1.

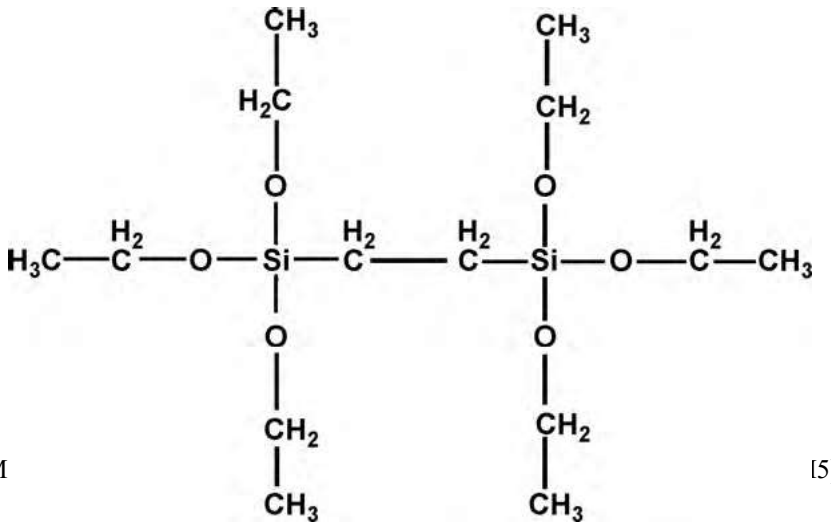

Figure.1 M [5) 6.

2.1. Wet Deposition

For wet deposition, 10% of the BTSE solution was diluted with water to 5% and then magnetically stirred for half an hour. The aluminum matrix was then pretreated, then immersed in the BTSE solution for 30 seconds and then the excess liquid was removed in dry air and treated for 2 hours in a furnace at 473 K for 2 hours.

2.2. Plasma deposition

2.2.1 Atmospheric pressure plasma

The atmospheric plasma device consists of a SurfX technology LLC, A-250D deposition system. Figure 2 shows the principle of a plasma torch (with a 5 cm2 shower head) [33]. The system operates at 13.56MHz frequency (RF), the plasma is formed by the transport of industrial argon, into the system, the upstream electrode flow rate of 30.0l / min, concentrated BTSE pioneer is stored in the temperature control at 373K, and was introduced into the plasma. The downstream electrode (after discharge) is bubbled through the liquid through the liquid pioneer. A homemade 3 cm diameter shower ring is used to get a uniform distribution of the pioneer. It consists of a 3mm diameter aluminum tube and 24 diameter of 1mm drill into the internal distribution of the tube around the regular composition (see Figure 2). The air flow is 0.5 cm downstream of the substrate. Plasma film deposition was performed at 80W for 2 minutes.

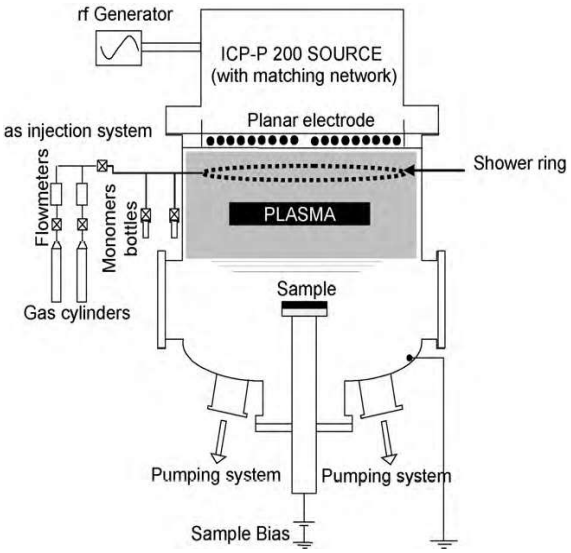

Figure 2

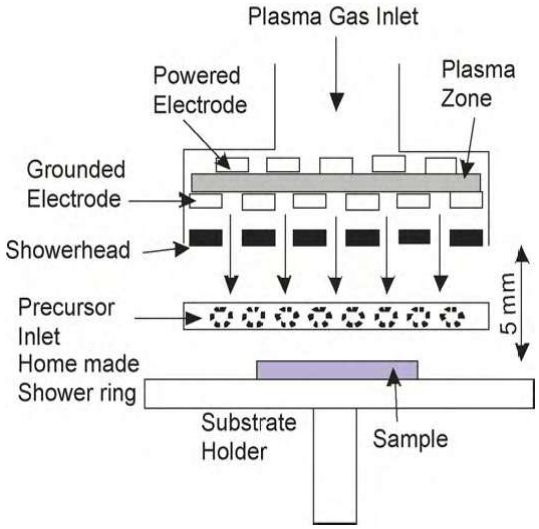

Figure 3

Figure 2 Schematic diagram of atmospheric plasma deposition apparatus.

Figure 3 Schematic diagram of a vacuum plasma reactor.

2.2.2 Vacuum Plasma

The vacuum plasma reactor (Figure 3) consists of three main parts: a planar source (ICP-P 200, JE PlasmaConsult GmbH, Germany), a gas injection system and a vacuum chamber.

The ICP-P 200 is radio frequency (13.56 MHz) inductive coupled plasma (ICP) source for a high density and low temperature plasma efficient production design. It consists of water-cooled four copper coil plane antenna (diameter of 20 cm), the electromagnetic power through a dielectric window (quartz) to the gas. It is run in an automatic mode, a radio frequency generator (Dressler® Cesar® 1310, Advanced Energy, Germany) and a reflection power of less than 2W within 10 seconds after the plasma is ignited.

The gas injection system consists of four flow meters (MKS1179A types), which are connected to a "Lin Yuhuan" output, allowing a uniform gas to be evenly distributed in the room. In the diameter of 20cm Lin Yuhuan by a diameter of 6mm stainless steel tube and 20 diameter of 1mm around the ring has a regular distribution of the drill into the internal holes.

The plasma chamber is connected to a pumping system (PFEIFFER DUO 20 MC 24m3 / h primary pump and PFEIFFER TPU 261 PC turbo molecular pump) with a 30 cm diameter stainless steel container. In the center of the vacuum chamber, the alumina cylinder is fixed on a four-axis manipulator. The sample holder is embedded in the stainless steel plate by alumina. A stainless steel rod with a diameter of 1 mm is inserted into the cylinder and connected to an electrical lead to apply the DC or RF bias on the sample if necessary. Otherwise, the sample may remain at the floating potential or ground. The distance between the sample and the quartz window can be adjusted from 0.5 to 17 cm. The pressure is based on the Convector p-type.

The sample was fixed to the sample stage by a carbon tape and placed in a plasma chamber, which was injected with 11 x 10-3 Torr pressure. The plasma is introduced into the plasma chamber by introducing the concentrated BTSE vapor monomer and polymerized through a valve to adjust the pressure to 300 mTorr. Polymerization is a continuous wave pattern where the deposition of the plasma film begins at 200W for 5 minutes and after discharge, the chamber pressure drops to 1 x 10-3 mTorr to avoid reaction of the remaining free radicals and external reactants after the reaction. In a vacuum or inert gas for 4 hours, and then transferred to the air to measure the photoelectron spectroscopy.

2.3. Surface Characterization

The X-ray photoelectron spectroscopy (XPS) was performed in the sample by means of a physical electron 5500 optoelectronic spectroscope. All spectra were collected with Mg Kα X-rays at 300W. Hyperspectral resolution of the spectrum through the use

23.5 electron volts are obtained, equivalent to a half full width (half width) at silver 3d5 / 2 1.05 eV peak. The binding ratio was calibrated by setting the main component at 284.4 eV of the C1 peak to complete [34].

BTSE film on aluminum (99.99%) of the Reflective Absorption Spectrometer (IRRAS) at 45 ◦

Wave number 2 cm-1 resolution, using a Nicolet 5700 FTIR equipped with an MCT detector measured by liquid nitrogen cooling spectrometer, infrared spectrum recorded and tested with 4000 to 650 cm-1. One hundred scan analysis to master the IRRAS data.

The surface morphology of the sample was described using a Japanese electron JSM - 7000F iron scanning electron microscope (field emission gun scanning electron microscope) with high spatial resolution. For the purpose of cross-sectional imaging, the silane sample is bent after immersion in liquid nitrogen, in order to ensure a substantial reduction in the film.

2.4. Electrochemical Impedance Spectroscopy (EIS)

The electrochemical impedance spectroscopy (EIS) is used to measure the frequency range of the OCP frequency range at 105 Hz to 10 MHz using the constant potential-AUTOLAB PGSTAT30 mode. The effective amplitude of the amplitude is 10mV, which consists of three electrode devices: an SCE reference, a platinum grid electrode, a working electrode, which is being studied by BTSE coated aluminum (effective area: 1.54 cm2). A platinum wire plus 10μF capacitor is placed parallel to the reference electrode to reduce the phase shift by the reference electrode in the high frequency range. These tests were carried out in 0.4 sodium sulfate solution.

3. Results and Discussion

3.1. film dip coating

The coated samples were transferred to the XPS analysis chamber and immediately deposited and cured. According to XPS analysis (Fig. 4, spectrum one), the outer surface of the film corresponds to the SiO1.7C region.

Binding and silicon percentages of the yard, oxygen and carbon present in the water-based BTSE film are given in Table 1, which contains 27.5% silicon, 45.8% oxygen and 26.7% carbon. The characteristic of the Si-O bond at 532.3 eV of the oxygen peak [34], the silicon peak at 102.3 eV for the R-siloxane type of silicon is expected to match the energy [34], the carbon peak at 284.4 eV, Significant C-O components.

Infrared Absorption Spectra of a Dip Coated Film

The peak at 1272 cm-1, the stretching of asymmetric Si-O-Si (1200 1000) cm-1 and the tetramethylation of the tetramethyl group at 800 cm-1 in Fig. 5 (spectrum A) and corresponding peak distribution table 2Si-CH3 Vibration observation. The oscillatory vibrations of the Si-O-C 1110cm-1 and CH2 are oscillating at (1000-1020) cm-1 in the possible four-CH2 silicon groups, the Si-O-Si stretching (1200-1000) cm- 1. The signal at 918 cm-1 can be determined as the Si-OH stretching vibration. Previous studies have shown that the heat curing at these layers increases the Si-O-H bond to the infrared absorption signal and increases the Si-O-Si bond [35], indicating that the condensation reaction

occurs between most of the silane layer molecules Cross-linked network. According to the observed electrochemical impedance spectroscopy, the formation of this network increases the barrier properties for hydrolysis and corrosion [35].

A water-based 5% BTSE membrane cross section is deposited by dip coating as shown in Fig. 6 with a film thickness of about 50 nm.

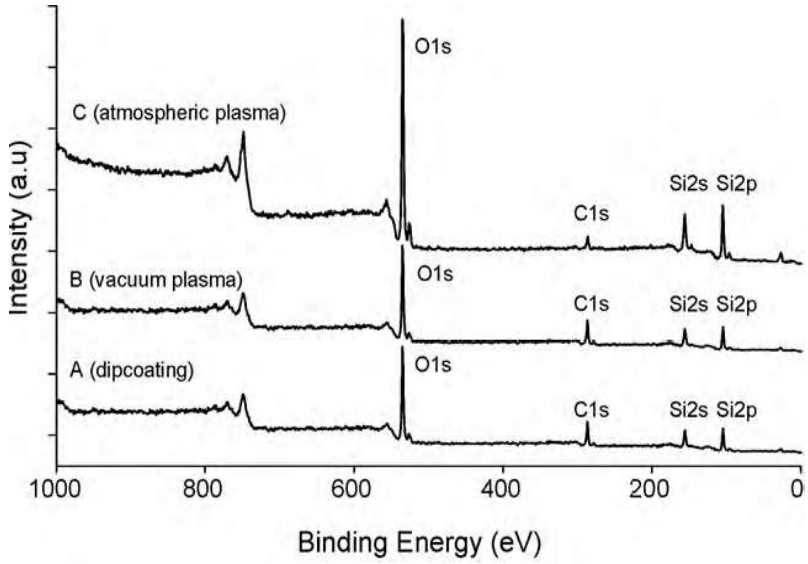

Figure 4 XPS spectrum deposition of BTSE film (A) Wet deposition, (B) Vacuum plasma and (C) Atmospheric plasma.

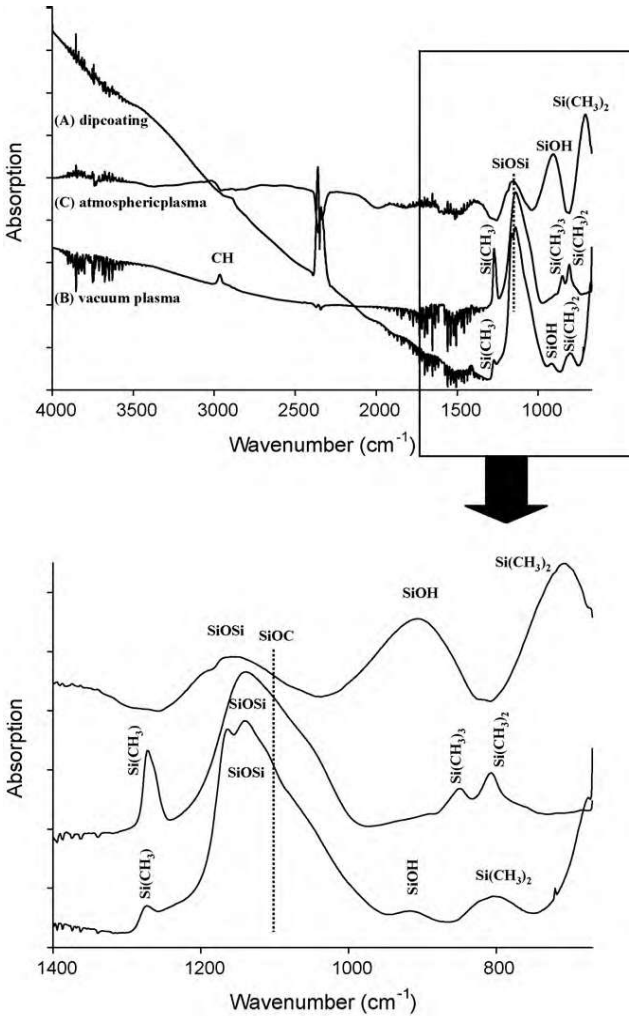

Figure 5 Infrared spectra of BTSE thin films deposited on aluminum (A) Wet deposition (B) Vacuum plasma (C) Atmospheric plasma.

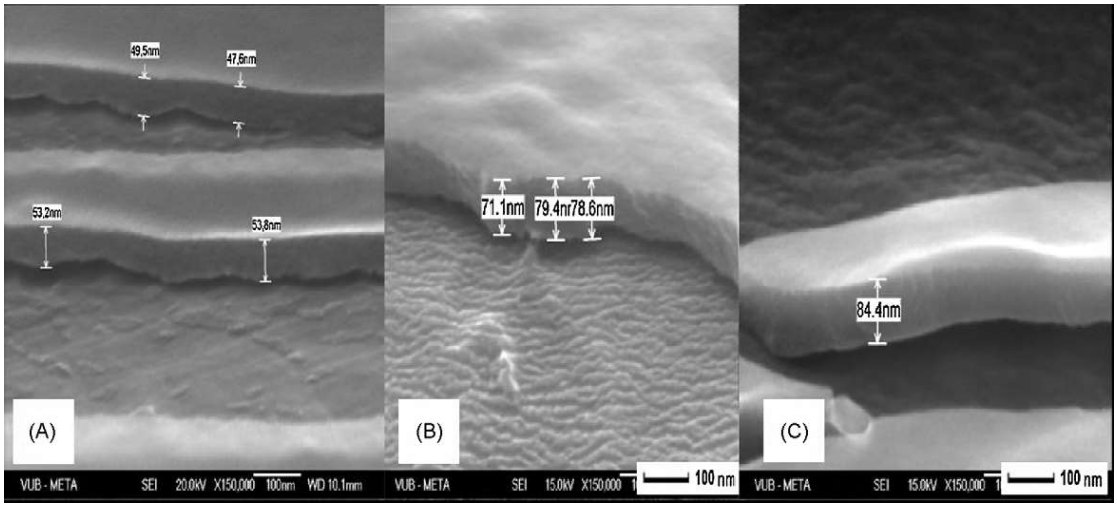

Figure 6 Cross-Bridging of Scanning Electron Microscopy (A) Wet deposition, (B) Vacuum plasma (C) Atmospheric plasma.

Table 1
Composition and binding energies of BTSE films as for XPS measurements.

	Binding energy (eV)			Atomic concentration (%)		
	Si_{2p}	C_{1s}	O_{1s}	Si_{2p}	C_{1s}	O_{1s}
Wet deposition	102.3	284.4	532.3	27.5	26.7	45.8
Vacuum plasma	102.7	284.4	532.3	28	24.3	47.6
Atmospheric plasma	103.2	284.4	532.8	34.7	6.7	58.6

3.2. Vacuum Plasma Deposition Film

The vacuum plasma XPS spectrum of the BTSE film is shown in Figure 4 (Spectrum B) and the elemental analysis results are reported in Table 1. The BTSE film contains Si, C, O, the peak of oxygen at 532.3 eV with Si-O bond characteristics [34], the silicon peak at 102.7 eV for the R-silicon ozone type silicone is expected to match the energy [34] , The peak of carbon at 284.4 eV is characteristic of C-C or C-H

The composition of the membrane is equivalent to SiO1.7C0.9 (Fig. 4, Spectrum B), compared to the unreacted BTSE precursor SiO3C7. The ratio of Si: O: C indicates that the formation of silicon - oxygen bonds and the Si - C bond during the process of the release of hydrocarbons.

Figure 5 (Spectrum B) gives the infrared spectrum of the plasma formed by the BTSE layer at a plasma deposition power of 200 W, 0.3 Torr, and a deposition time of 5 min. The peak distribution is shown in Table 2. It reveals a large number of dimethyl silyl groups.

(Si-O-Si) in the presence of (1200-1000) cm-1, dimethylsilyl (Si- (CH3) 2) at 806 cm-1 and trimethylsilyl (Si-) Is clearly visible at 850 cm-1. The telescopic vibration leads to the conclusion that the concentration of CH2 is quite low (see Fig. 7).

Figure 6B shows a scanning electron micrograph of a BTSE film deposited by vacuum plasma on a cross section of an aluminum substrate. The film is continuously compact about 70 nanometers thick. The plasma execution process results in a homogeneous membrane.

Table 2
IRRAS peak assignment for the BTSE films.

	Wave number (cm^{-1})	Group	Assignment
Wet deposition	1272	$Si–CH_3$	$\delta_s(CH_3)$
	1200–1000	Si–O–Si	ν_{as}(Si–O–Si)
	1110	Si–O–C	ν_{as}(Si–O–C)
	1020–1000	$SiCH_2–Si$	CH_2 wagg.
	918	Si–OH	δ_s(SiOH)
	800	$Si–(CH_3)_2$	r(Si–CH_3)
Vacuum plasma	1270	$Si–CH_3$	$\delta_s(CH_3)$
	1200–1000	Si–O–Si	ν_{as}(Si–O–Si)
	1110	Si–O–C	ν_{as}(Si–O–C)
	1020–1000	$SiCH_2–Si$	CH_2 wagg.
	850	$Si–(CH_3)_3$	r(Si–CH_3)
	806	$Si–(CH_3)_2$	r(Si–CH_3)
Atmospheric plasma	1250–1000	Si–O–Si	ν_{as}(Si–O–Si)
	912	Si–OH	δ_s(SiOH)
	712	$Si–(CH_3)_2$	r(Si–CH_3)

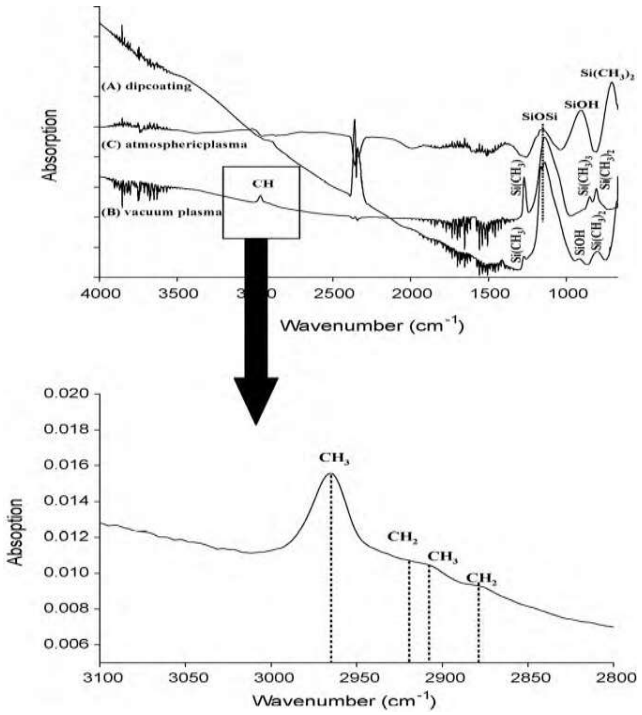

Figure 7 BTSE film deposition of vacuum plasma polymer infrared reflection absorption spectrum.

3.3. Deposition by atmospheric plasma

Membrane deposition plasma power from 40 to 100W, deposition time from 2 to 30 minutes at atmospheric pressure. Only the 80W XPS and IRRAS spectra were loaded because of the no effect of the composition and structure of the film observed with different power and deposition time. In fact, the infrared spectra recorded in these different power synthesis' will not reveal any bands and peak energy and relative intensity changes in the sample, presented in a similar chemical film. Due to the particularity of the plasma process, the deposition time is only affected by the thickness of a pair of deposited films.

The binding energy and the current percentage of silicon, oxygen and carbon atoms in the film are listed in Table 1, due to the XPS analysis results. The membrane consists of 34.7% silicon, 58.6% oxygen and 6.7% carbon. Oxygen at 532.8 eV of the characteristic peaks observed in (1250 to 1000 years) cm - 1. The 912cm-1 band is also visible, showing the presence of Si-OH.

A representative BTSE film is deposited on the atmospheric plasma as shown in Figure 6C, with a thickness of about 80 nanometers (deposition time of 30 minutes). The atmospheric plasma process also results in a uniform terrain film.

Table 3
Fitting data from XPS analysis of BTSE films.

Element (peak)	Predominant oxidation states (location of peak maximum)		
	Dipcoating	Vacuum plasma	Atmospheric plasma
Si_{2p}	+II (102.3 eV)	+III (102.7 eV)	+III, +IV (103.2 eV)
C_{1s}	0 (284.4 eV)	0 (284.4 eV)	0 (284.4 eV)
O_{1s}	−II (532.3 eV)	−II (532.3 eV)	−II (532.8 eV)

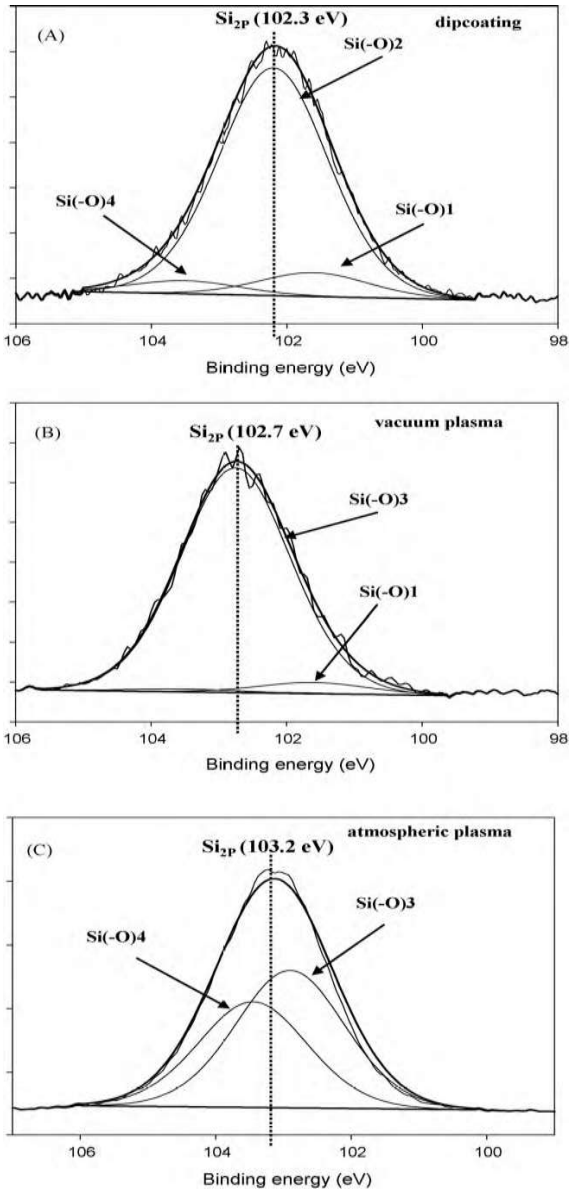

Figure 8 shows the XPS high resolution (Si2p.)

(A)BTSE wet deposition, (B) Vacuum plasma and (C) Atmospheric plasma

3.4. Comparison of membrane deposition under different techniques

Table 1 summarizes the XPS analysis of the film and the deposition of three methods. While the values related to the dip coating and the vacuum plasma film are comparable, the C/O ratio of the atmospheric plasma BTSE film decreases from 26.7 to 6.7% from 0.6 to 0.1. The silicon content on the surface of the film, on the other hand, increased the dip coating and vacuum plasma from 27.5%, deposited on the film at 34.7% atmospheric pressure plasma.

The Si2p atmospheric plasma film has a higher binding than expected, showing a value (103.2 eV) that is consistent with the IRRAS measurement. In fact, from the XPS data show that the BTSE film of atmospheric plasma than those using vacuum plasma oxidation and dip coating deposition, and the corresponding infrared spectra show that the transition of silicon O-Si at 1250 -1000 cm-1 stretching vibration, High oxidation state. In contrast, the 1270 cm-1 Si-methyl band attenuation indicates that the methyl group and the corresponding monoxide removal of the carbon atom concentration are reduced by X-ray photoelectron spectroscopy. The absence of a 2950cm-1 stretch on a C-H bond also provides evidence of the atmospheric pressure plasma of the film on the preferential loss of organic matter.

The characteristics of the BTSE film are also studied using the curve of the Si2p core layer peak fitting. The Si2p peak is decomposed into four components (Figure 8) according to the method described by Alexander et al. [34]. The peak of the evolution shown in Table 3. At 102.1 ± 0.1 eV is assigned to the component bound to two oxygen atoms of silicon R2Si (- O) 2 [34] at 102.8 ± 0.1 eV to the component bound to the three oxygen atoms of the silicon R2Si (-O) 3 [34] and at 103.4 ± 0.1 eV are necessarily bound to be assigned to four oxygen atoms of silicon (-O) 4 [34]. The BTSE film was dip deposited on the composition of R2Si (-O) by 2 86% while the plasma BTSE film was the main component of vacuum plasma deposition of R2Si (-O) 3 (94%). R2Si (-O) 3 and silicon oxide modules (-O) deposited on the plasma BTSE film at atmospheric pressure were 56.5% and 43.4%, respectively,

Carbon and oxygen concentrations increase in atmospheric settling. Si-O bonds are more abundant than those of the rich deposition by vacuum plasma oxide film formation and dip. The electrochemical impedance spectroscopy was carried out by preliminary dip coating samples to examine how the presence of BTSE affected the barrier properties of the bare substrate. The test was immersed in NaSO4 and the focus was on the middle of their frequency range, in this type of coating barrier properties, usually found [36] behaviorally concentrated samples.

Figure 9 shows the impedance modulus (Bode plot) of the uncoated substrate (by its characteristic native alumina cap) and the substrate inclination with the BTSE coating. A significant difference can be observed in the frequency range of the two samples (the circle part in the figure). It is a uniform aluminum that is covered by a soaked silane layer, thus ensuring good barrier properties. EIS testing is underway and has not yet been carried out on atmospheric and vacuum plasma silane membranes. The results of the preliminary electrochemical impedance spectroscopy on the sample and the results of the above investigation are better based on the performance of the barrier properties are expected to be in the plasma deposition coating, especially due to atmospheric plasma, high cross-linking of the above proof results.

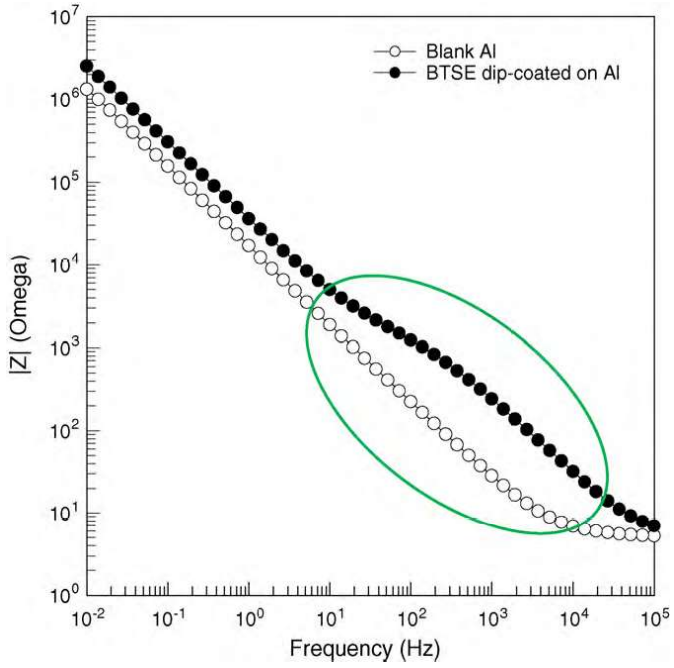

Figure 9 The base of the blank sample impedance (Bode representation) modulus sum

One sample is impregnated with BTSE coating.

4. Conclusion

The object of this study is that each BTSE film is deposited with three different techniques: dip (waterborne silane), vacuum plasma and atmospheric plasma. Atmospheric and vacuum ion plating films BTSE has never been reported in the literature. XPS and infrared spectroscopy measurements show that the presence of silicon in the siloxane layer is different. IRRAS highlights groups such as Si-O-Si bonds, Si-O bond-C and Si-O bonds and Si-CH3 groups.

XPS is used to quantify silicon coatings in different environments. A high proportion is obtained in the Si (-O) 2 environment for soaking the coating. The silicon atoms in the plasma BTSE films were vacuum deposited in Si (O) in three environments. Atmospheric plasma method, 43% of the silicon atoms in the silicon (-O) 4 environment, 57% are three oxygen bonds (Si (-O) 3). The vacuum plasma deposition layer can be considered more organic - inorganic film, comparable to that obtained by dip coating of the silane film. However, atmospheric plasma treatment leads to the

formation of oxide films that are richer than Si-O bonds, which are more inorganic than those deposited using vacuum plasma and inorganic coating.

References

1. A.M. Beccaria, L. Chiartini, Corros. Sci. 41 (1999) 885.
2. A. Cabral, R. G. Duarte, M. F. Montemor, M.L. Zheludkevich, M. G.S. Ferreira, Corros. Sci. 47 (3) (2005) 869.
3. V. Palanivel, D.Q. Zhu, W.J. van Ooij, Prog. Org. Coat. 47 (2003) 384.
4. W. Trabelsi, L. Dhouibi, E. Triki, M. G.S. Ferreira, M.F. Montemor, Surf. Coat. Technol. 192 (2/3) (2005) 284.
5. V. Subramanian, W.J. van Ooij, Corrosion 54 (1998) 204.
6. J.-M. Hu, L. Liu, J.-Q. Zhang, C.-N. Cao, Electrochim. Acta 51 (2006) 3944.
7. C.M. Bertelsen, F.J. Boerio, Prog. Org. Coat. 41 (2001) 239.
8. R. d'Agostino (Ed.), Plasma Processing of Polymers, NATO ASI Series, Kluwer Academic Publishers, 1997.
9. E.P. Plueddemann, Silane Coupling Agents, 2nd ed., Plenum Press, New York, 1990.
10. A. Franquet, Characterization of silane films on aluminum, Ph.D. Thesis in Department of metallurgie Electrochemistry and Materials Science, Vrije Universiteit Brussel, Brussels, 2002.
11. M.G.S. Ferreira, R. G. Duarte, M.F. Montemor, A.M.P. Simoes, Electrochim. Acta 49 (2004) 2927.
12. K. Aramaki, Corros. Sci. 41 (1999) 1715.
13. A. Pepe, M. Aparicio, S. Céeré, A. Durán, J. Non-Cryst. Solids 348 (2004) 162.
14. V. Palanivel, Y. Huang, W.J. van Ooij, Prog. Org. Coat. 53 (2005) 153.
15. M. Sheffer, A. Groysman, D. Starosvetsky, N. Savchenko, D. Mandler, Corros. Sci. 46 (2004) 2975.
16. A. Phanasgaonkar, V.S. Raja, Surf. Coat. Technol. 203 (2009) 2260-2271.
17. M.F. Montemor, R. Pinto, M. G.S. Ferreira, Electrochim. Acta 54 (2009) 5179-5189.
18. M.F. Montemor, A.M. Simoes, M.G.S. Ferreira, Prog. Org. Coat. 44 (2) (2002) 111-120.
19. M.F. Montemor, et al., Prog. Org. Coat. 57 (2006) 67-77.
20. W. Trabelsi, et al., Prog. Org. Coat. 54 (2005) 276-284.
21. K.A. Yasakau, et al., J. Phys. Chem. 110 (2006) 5515-5528.
22. D. Zhu, W.J. Van Ooij, Prog. Org. Coat. 49 (2004) 42.
23. C. Tendero, C. Tixier, P. Tristant, J. Desmaison, P. Leprince, Spectrochim. Acta B 61 (2006) 2.
24. A.M.Wrobel, M. R. Wertheimer, J. Dib, H.P. Schreiber, J. Macromol. Sci. Chem. A (3) (1980) 321.
25. N. Inagaki, M. Taki, J. Appl. Polym. Sci. 27 (1982) 4337.
26. A. Sabata, W.J. van Ooij, H.K. Yasuda, Surf. Interface Anal. 20 (1993) 845.
27. K. G. Sachdev, H. Sachdev, Thin Solid Films 107 (3) (1983) 245.
28. I. Tajima, M. Yamamoto, J. Polym. Sci. A: Polym. Chem. 25 (7) (1987) 1737.
29. V. Barbarossa, S. Contarini, A. Zanobi, J. Appl. Polym. Sci. 44 (11) (1992) 1951.
30. T. Hiraide, H. Yamada, O. Tsuji, J. Photopolym. Sci. Technol. 7 (2) (1994) 45
31. P. Supiot, C. Vivien, A. Granier, A. Bousquet, A. Mackova, D. Escaich, R. Clergereaux, P. Raynaud, Z. Stryhal, J. Pavlik, Plasma Process. Polym. 2) (2006) 100.
32. R. Prikryl, V.Cech, R. Balkova, J. Vanek, Surf. Coat. Technol. 173-174 (2003) 858.
33. A. Ladwig, S. Babayan, M. Smith, M. Hester, W. Highland, R. Koch, R. Hicks, Surf. Coat. Technol. 201 (2007) 6460.
34. M.R. Alexander, R.D. Short, F. R. Jones, W. Michaeli, C. J. Blomfield, Appl. Surf. Sci. 137 (1999) 179-183.
35. I. De Graeve, J. Vereecken, A. Franquet, T. Van Schaftinghen, H. Terryn, Prog. Org. Co. 59 (2007)
36. T. Van Schaftinghen, C. Le Pen, H. Terryn, F. Horzenberger, Electrochim. Acta 49 (2004) 299